Journal of Computational and Applied Mathematics 234 (2010) 1876–1885

Contents lists available at ScienceDirect

Journal of Computational and Applied Mathematics

journal homepage: www.elsevier.com/locate/cam

Homogenization of the acoustic transmission through a perforated layer[☆]

E. Rohan[*], V. Lukeš

Department of Mechanics, Faculty of Applied Sciences, UWB in Pilsen, Univerzitní 22, 306 14 Plzeň, Czech Republic
New Technologies Research Center, UWB in Pilsen, Univerzitní 22, 306 14 Plzeň, Czech Republic

ARTICLE INFO

Article history:
Received 12 December 2007
Received in revised form 12 November 2008

Keywords:
Acoustic transmission
Perforated duct
Two-scale homogenization
Homogenized impedance

ABSTRACT

The paper deals with homogenized transmission conditions imposed on an interface plane separating two halfspaces occupied by an acoustic medium. The conditions are obtained as the two-scale homogenization limit of a standard acoustic problem imposed on the layer perforated by a sieve-like obstacle with a periodic structure. Both the characteristic scale of the perforations and the layer thickness are parametrized by $\varepsilon \to 0$. The limit model involving some homogenized coefficients governs the interface discontinuity of the acoustic pressure associated with the two halfspaces and the magnitude of the transverse acoustic velocity. This novel approach allows for the treatment of complicated designs of perforations and presents an alternative to the usual description of acoustic impedance, which relies on a rough averaging of the quasi-experimental data.

1. Introduction

The design of noise reducing devices is an important challenge in automotive engineering, which in particular may diminish in part, the acoustic pollution produced by combustion engines. Apart from the optimization of exhaust silencers, obviously, there are other devices involving sieve-like structures for which acoustic transmission is an important process to be analyzed.

Waves propagating in the acoustic medium with periodically embedded obstacles could be studied numerically using the finite element method, without imposing any additional transmission conditions, if the FE mesh were refined enough in the interface layer containing the obstacles. However, the complexity of such brute-force models would be intractable, especially if an inverse problem of optimal design is in mind. Therefore, it is natural to represent the real perforated interface by a hyperplane where the interface transmission condition can be prescribed. The purpose of the paper is to present the homogenization approach employed to derive a proper model of acoustic transmission through a perforated planar structure.

We consider the acoustic medium occupying domain Ω^G which is subdivided by a perforated plane Γ_0 into two disjoint subdomains Ω^+ and Ω^-, so that $\Omega^G = \Omega^+ \cup \Omega^- \cup \Gamma_0$; see Fig. 1 (left). Denoting by p^+ and p^- the acoustic pressures in Ω^+ and Ω^-, respectively, in a case of no convection flow, the acoustic waves in Ω^G are described by the following equations

$$
\begin{aligned}
& c^2\nabla^2 p^+ + \omega^2 p^+ = 0 \quad \text{in } \Omega^+, \\
& c^2\nabla^2 p^- + \omega^2 p^- = 0 \quad \text{in } \Omega^-, \\
& + \text{boundary conditions} \quad \text{on } \partial\Omega^G,
\end{aligned}
\tag{1}
$$

supplemented by the transmission conditions on the interface Γ_0—these represent *the key issue of this paper.*

☆ This research and publication were supported by projects GAČR 101/07/1471 and MSM 4977751301 of the Czech Republic.
* Corresponding author at: Department of Mechanics, Faculty of Applied Sciences, UWB in Pilsen, Univerzitní 22, 306 14 Plzeň, Czech Republic.
E-mail address: rohan@kme.zcu.cz (E. Rohan).

0377-0427/$ – see front matter
doi:10.1016/j.cam.2009.08.059

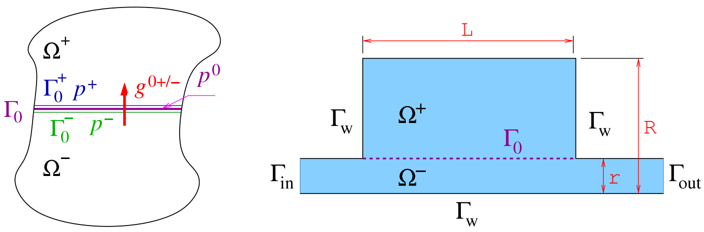

Fig. 1. Left: the scheme of the interface transmission coupling the acoustic pressure jump and the transverse velocity proportional to g^0. Right: the domain and boundary decomposition of the global acoustic problem considered in the numerical examples, $L = 1$ m, $r = 0.12$ m, $R = 0.47$ m; this design is inspired by [2].

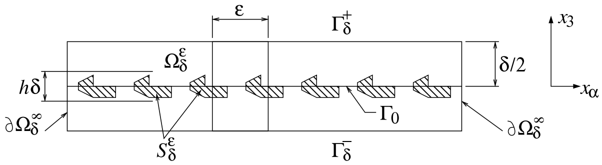

Fig. 2. The layer Ω_δ of the acoustic medium with periodic "solid perforations" S_δ^ε situated within the layer $x_3 \in]-h\delta/2, +h\delta/2[$, where $h < 1$. The reference periodic cell spans the whole thickness of the layer.

The standard treatment of the acoustic transmission on perforation Γ_0 results in the relationship between jump $p^+ - p^-$ and normal derivatives $\frac{\partial p^+}{\partial n^+} = -\frac{\partial p^-}{\partial n^-}$,

$$\frac{\partial p^+}{\partial n^+} = -\mathrm{i}\frac{\omega\rho}{Z}(p^+ - p^-), \qquad \frac{\partial p^-}{\partial n^-} = -\mathrm{i}\frac{\omega\rho}{Z}(p^- - p^+), \tag{2}$$

where n^+ and n^- are the outward unit normals to Ω^+ and Ω^-, respectively, ω is the frequency, ρ is the density and Z is the *transmission impedance*; this complex number is characterized by features of the actual perforation considered and is determined semi-empirically using an averaging procedure and experiments in the acoustic laboratories, see e.g. [1].

Recently, the problem of acoustic transmission in the muffler structure was studied in [3,2] by means of the asymptotic method; the acoustic pressure in the layer surrounding the perforation is described in terms of so-called inner and outer expansions associated with the tangent and normal directions w.r.t. the layer mid-surface. Although this model seems to provide a very good approximation for usual type of sieves formed as plate drilled by cylindrical holes, its extension for more complicated types of perforation is not clear.

We suggest a more refined mathematical treatment of the transmission condition where quite general shapes of periodic perforations are considered. More precisely, rather than $(p^+ - p^-)/Z$, see (2), the resulting conditions involve g^0, the acoustic momentum, which is related to $p^+ - p^-$ by means of the *homogenized interface layer problem* involving several *homogenized coefficients*; these can be computed directly for a specified shape of the perforation. As an advantage, with such modelling approach one can think of *inverse problems* aimed at the optimal design of the perforated structure to obtain a desired acoustic response.

The outline of the paper appears as follows. In Section 2.1 we explain how the geometry of the perforated transmission layer depends on scale parameter ε and formulate the Neumann problem describing the acoustic pressure distribution driven by the transverse acoustic velocities. The homogenization procedure is presented in an abbreviated form in Section 3 where we define the local problems and the homogenized coefficients involved in the transmission layer problem. This provides the acoustic impedance constituting the transmission condition imposed on the perforated surface in the global problem formulation, as discussed in Section 4. Finally, in Section 5 we introduce some illustrative numerical examples of 2D problems of acoustic transmission, showing influence of the perforation design.

2. Problem formulation

We shall now consider acoustic waves in the layer $\Omega_\delta \subset \mathbb{R}^3$ representing a small neighbourhood of the interface Γ_0, where ultimately the transmission conditions for problem (1) will be supplied as the result of the homogenization procedure. Ω_δ is featured by its finite thickness δ and generated by a planar mid-surface Γ_0 parallel with axes directions $\alpha = 1, 2$. The layer is occupied in part by the acoustic medium (inviscid fluid) and in part by a perforated slab where the acoustic medium penetrates. The slab is a plate-like rigid sieve characterized by the thickness $h\delta$, $h < 1$ and by a periodic perforation, see Fig. 2 where a section through the layer is illustrated.

Here we briefly introduce the acoustic problem depending on small parameter ε; asymptotic analysis of this problem leads to a homogenized model describing acoustic wave propagation in such a thin layer. In the context of the global problem outlined in the Introduction, this homogenized model will replace interface conditions (2).

Notation. By index $^\varepsilon$ we denote dependence of variables on scale parameter $\varepsilon > 0$; similar convention is adhered in the explicit reference to $\delta > 0$. By the Greek indices we refer to the coordinate index 1 or 2, so that $(x_\alpha, x_3) \in \mathbb{R}^3$. By y we refer to triplet $(y_\alpha, z) \in \mathbb{R}^3$. The Einstein summation convention for repeated indices is employed.

2.1. Geometry

Let $\Gamma_0 \subset \mathbb{R}^2$ be an open bounded subdomain of the plane spanned by coordinates x_α, $\alpha = 1, 2$ and containing the origin. Further let Γ_δ^+ and Γ_δ^- be equidistant to Γ_0 with the distance $\delta/2 = \mathrm{dist}(\Gamma_0, \Gamma_\delta^+) = \mathrm{dist}(\Gamma_0, \Gamma_\delta^-)$. We introduce $\Omega_\delta = \Gamma_0 \times]-\delta/2, \delta/2[\subset \mathbb{R}^3$, an open domain representing the transmission layer bounded by $\partial\Omega_\delta$ which is split as follows

$$\partial\Omega_\delta = \Gamma_\delta^+ \cup \Gamma_\delta^- \cup \partial\Omega_\delta^\infty, \qquad \Gamma_\delta^\pm = \Gamma_0 \pm \frac{\delta}{2}\vec{e}_3, \qquad \partial\Omega_\delta^\infty = \partial\Gamma_0 \times]-\delta/2, \delta/2[, \tag{3}$$

where $\delta > 0$ is the layer thickness and $\vec{e}_3 = (0, 0, 1)$, see Fig. 2. The acoustic medium occupies domain $\Omega_\delta^\varepsilon = \Omega_\delta \setminus \overline{S_\delta^\varepsilon}$, where S_δ^ε is the solid-*rigid* obstacle which in a simple layout has a form of the periodically perforated sheet with the thickness $h\delta$, $h < 1$; thus, S_δ^ε is obtained by the usual *periodic lattice* extension of the solid unit structure.

We would like to stress out, that in *our treatment*, the solid-rigid structures S_δ^ε are periodic w.r.t. the tangential direction relative to Γ_0 and the domain of interest, Ω_δ, is restricted by the finite thickness. This is the *major difference* with the approaches reported in [3,2] or in [4,5], cf. [11] Chapter 17, where the domains consisted from ribs "elongated" to infinity in the normal direction to Γ_0 and the solid-rigid structures were only infinitely thin perforated sheets, i.e. periodic "obstacles" embedded in Γ_0.

In the homogenization procedure we shall use the *dilatation technique* to transform the problem into a fixed domain, cf. [6]. Therefore, $x_3 \in]-\delta/2, \delta/2[$ and we introduce the rescaling $x_3 = z\delta$ so that one has $z \equiv y_3 \in]-1/2, +1/2[$.

2.2. Acoustic transmission in the finite thickness layer

Assuming no convection flow of the medium the total acoustic pressure, $p^{\varepsilon\delta}$, varying with frequency ω satisfies the Helmholtz equation in $\Omega_\delta^\varepsilon$ and Neumann condition on $\partial\Omega_\delta$

$$\begin{aligned} &c^2\nabla^2 p^{\varepsilon\delta} + \omega^2 p^{\varepsilon\delta} = 0 \quad \text{in } \Omega_\delta^\varepsilon, \\ &c^2\frac{\partial p^{\varepsilon\delta}}{\partial n^\delta} = -\mathrm{i}\omega g^{\varepsilon\delta\pm} \quad \text{on } \Gamma_\delta^\pm, \\ &\frac{\partial p^{\varepsilon\delta}}{\partial n^\delta} = 0 \quad \text{on } \partial S_\delta^\varepsilon \cup \partial\Omega_\delta^\infty, \end{aligned} \tag{4}$$

where $c = \omega/k$ is the speed of sound propagation and by n^δ we denote the normal vector outward to Ω_δ, so that due to the special choice of the coordinate system:

$$\frac{\partial}{\partial n^\delta} = \frac{\partial}{\partial x_3} = \frac{1}{\delta}\frac{\partial}{\partial z}\ .$$

In (4) $g^{\varepsilon\delta\pm} = c^2\rho_0 v_{n0}$, where v_{n0} is the amplitude of the normal velocity and ρ_0 is the reference density, so that $g^{\varepsilon\delta\pm}/c^2$ is the interface normal momentum. This quantity is subject to additional assumptions introduced in Section 3.1.

After the thickness dilatation $x_3 = \delta z$, see Fig. 3, the problem is transformed in domain $\Omega^{*\varepsilon} \subset \Omega = \Gamma_0 \times]-1/2, 1/2[$ with the unit (constant) thickness. Functions defined in the dilated domain will be labelled by superscript ε, instead of $\varepsilon\delta$. The weak formulation of (4) then reads as follows: find $p^\varepsilon \in H^1(\Omega^\varepsilon)$ such that

$$c^2\int_{\Omega^{*\varepsilon}}\left(\partial_\alpha p^\varepsilon\partial_\alpha q + \frac{1}{\delta^2}\partial_z p^\varepsilon\partial_z q\right) - \omega^2\int_{\Omega^{*\varepsilon}} p^\varepsilon q = -\mathrm{i}\omega\frac{1}{\delta}\left(\int_{\Gamma^+} g^{\varepsilon+}q\,\mathrm{d}\Gamma + \int_{\Gamma^-} g^{\varepsilon-}q\,\mathrm{d}\Gamma\right) \quad \text{for all } q \in H^1(\Omega^{*\varepsilon}). \tag{5}$$

3. Homogenization

For passing to the limit $\varepsilon \to 0$ we consider a proportional scaling between the period length and the thickness, so that $\delta = \varkappa\varepsilon$, where $\varkappa > 0$ is fixed.

The homogenized coefficients governing the acoustic transmission are introduced below using so-called corrector functions defined in the reference periodic cell $Y =]0, 1[^2 \times]-1/2, +1/2[\subset \mathbb{R}^3$. The acoustic medium occupies domain $Y^* = Y \setminus S$, where $S \subset Y$ is the solid (rigid) obstacle, see Fig. 3. For clarity we use notation $I_y =]0, 1[^2$ and $I_z =]-1/2, +1/2[$. The upper and lower boundaries are translations of $(I_y, 0)$; we define $I_y^+ = \{y \in \partial Y : z = 1/2\}$ and $I_y^- = \{y \in \partial Y : z = -1/2\}$. By $H^1_{\#(1,2)}(Y)$ we denote the space of $H^1(Y)$ functions which are "1-periodic" in coordinates y_α, $\alpha = 1, 2$; in this paper such functions will be called "transversely Y-periodic".

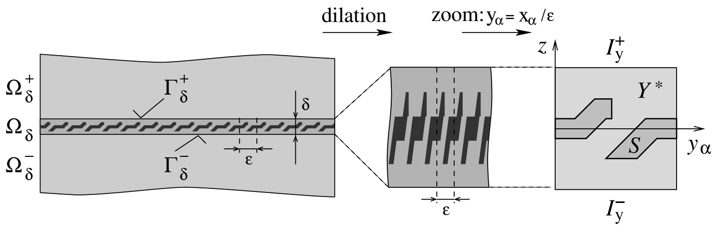

Fig. 3. The perforated interface layer, Ω_δ embedded in Ω^G; illustration of the thickness *dilatation* and of zooming in the *periodic structure* by factor $1/\varepsilon$ in x_α coordinates. The perforation geometry is then represented by $Y^* \subset Y$.

3.1. Homogenization procedure

The model presented in this paper was derived originally using the *periodic unfolding method* of homogenization, cf. [7,8], which, however, is relatively new and not frequently used so far. Therefore, in order to justify the homogenization result, we shall briefly describe an alternative method of homogenization based on the Tartar method of oscillating functions. In fact, the procedure applied in [6], Chapter 3, Section 2.1, can be adapted easily to the present problem which is characterized by the following assumptions. We need convenient prepositions on the limit fluxes acting on $\Gamma_\delta^\pm$, or on $\Gamma^\pm$ in the dilated configuration. Let us introduce *shifted* fluxes $\hat{g}^{\varepsilon\pm} \in L^2(\Gamma_0)$ such that $\hat{g}^{\varepsilon\pm}(\bar{x}) = g^{\varepsilon\pm}(x^\pm)$ where $x^\pm \in \Gamma^\pm$ are homologous points associated to $\bar{x} \in \Gamma_0$, i.e. $\bar{x} = (\bar{x}_\alpha, 0)$ and $x^\pm - \bar{x} = (0, 0, \pm 1/2)$. We assume

$$\hat{g}^{\varepsilon\pm} \rightharpoonup g^{0\pm} \quad \text{weakly in } L^2(\Gamma_0), \tag{6}$$

$$\frac{1}{\varepsilon}\left(\hat{g}^{\varepsilon+} + \hat{g}^{\varepsilon-}\right) \rightharpoonup 0 \quad \text{weakly in } L^2(\Gamma_0), \tag{7}$$

consequently $g^0 \equiv g^{0+} = -g^{0-}$. This equality means continuity of the normal momentum, which is consistent with the consequence of (2). Assumption (7) may be weakened in the sense that $(\hat{g}^{\varepsilon+} + \hat{g}^{\varepsilon-}) \approx O(\varepsilon)$, so that the a priori estimation (see Step 1 below) still can be obtained; this will be issued in a forthcoming publication.

The homogenization procedure is based on the following steps: (1) a priori estimation of the pressure gradient, which gives the "hint" for (2) the formal asymptotic expansion; using this procedure one obtains a pressure corrector, p^1 and its decomposed form which reveals the local auxiliary problems and the global homogenized problem; (3) using the Tartar variational method convergence of the pressure gradient is proved and the homogenized coefficients identified; (4) a finite scale of the obstacle thickness and, thereby, of the interface layer Ω_{δ_0} with $\delta_0 > 0$ must be considered, which leads to a modification of the homogenization result. We shall now specify the main spirit of these steps.

In what follows we denote by $\hat{\nabla}^\varepsilon$ and $\hat{\nabla}$ the gradients in the dilated coordinate systems:

$$\nabla \equiv (\partial_1^x, \partial_2^x, \partial_3^x) = \hat{\nabla}^\varepsilon \equiv \left(\partial_\alpha^x, \frac{1}{\varkappa\varepsilon}\partial_z\right) = \frac{1}{\varepsilon}\hat{\nabla}_y \equiv \frac{1}{\varepsilon}\left(\partial_\alpha^y, \frac{1}{\varkappa}\partial_z\right). \tag{8}$$

Step 1: We assume provisionally that $\|p^\varepsilon\|_{L^2(\Omega^\varepsilon)} \le C$, where from now on C is a constant independent of ε; this assumption is justified afterwards following a similar approach employed in [9], once the strong convergence of p^ε in $L^2(\Omega)$ is obtained. Due to (6)–(7) one obtains $\|\partial_\alpha p^\varepsilon\|_{L^2(\Omega^\varepsilon)} \le C$ and $\|\partial_z p^\varepsilon\|_{L^2(\Omega^\varepsilon)} \le \varepsilon\varkappa C$. On introducing a smooth prolongation operator, see e.g. [6], Chapter 1, $\mathcal{P}_\Omega : H^1(\Omega^{*\varepsilon}) \to H^1(\Omega)$, where $\Omega^{*\varepsilon} = \Omega \setminus S^\varepsilon$, and using the above estimates the following convergences are evident:

$$\begin{aligned} &\mathcal{P}_\Omega p^\varepsilon \rightharpoonup p^0 \quad \text{weakly in } H^1(\Omega), \\ &\partial_z \mathcal{P}_\Omega p^\varepsilon \rightharpoonup 0 \quad \text{weakly in } L^2(\Omega), \end{aligned} \tag{9}$$

hence $\mathcal{P}_\Omega p^\varepsilon \to p^0$ strongly in $L^2(\Omega)$ and $p^0(x_\alpha, z) = p^0(x_\alpha)$, i.e. $\partial_z p^0 = 0$. In what follows we use abbreviation $\mathcal{P}_\Omega p^\varepsilon = \tilde{p}^\varepsilon$. Recalling the original problem of interest specified in the Introduction, Ω_δ may be embedded in a larger domain $\Omega' \supset \Omega_\delta$ where p^ε is defined (possibly $\Omega' = \Omega^G$). Let $\gamma_\delta^\pm(p^{\varepsilon\delta})$ be the trace of $p^{\varepsilon\delta}$ from $\Omega_\delta^\pm$ on $\Gamma_\delta^\pm$ (i.e. from outside of Ω_δ). Further we assume the weak convergence $\gamma_\delta^\pm(p^{\varepsilon\delta}) \rightharpoonup p^\pm$ in $L^2(\Gamma_0)$; for any $\phi \in L^2(\Omega')$ constrained by $\partial_3\phi = 0$ it holds that

$$\int_{\Omega^\delta} \phi\partial_3\widetilde{p^{\varepsilon\delta}} = \int_{\Gamma_\delta^+} \phi\gamma_\delta^+(p^{\varepsilon\delta})\mathrm{d}\Gamma - \int_{\Gamma_\delta^-} \phi\gamma_\delta^-(p^{\varepsilon\delta})\mathrm{d}\Gamma \overset{\delta,\varepsilon\to 0}{\longrightarrow} \int_{\Gamma_0} \phi(p^+ - p^-)\mathrm{d}\Gamma. \tag{10}$$

Step 2: Further we may consider all gradients $\partial_\alpha^x p^\varepsilon$, $\partial_z p^\varepsilon$ extended by zero in $\Omega \setminus \Omega^{*\varepsilon} = S^\varepsilon$. In (5) we employ formal asymptotic expansions: $p^\varepsilon = p^0(x_\alpha) + \varepsilon p^1(x_\alpha, y) + \dots, y \in Y^*$, with $p^0 \in H^1(\Gamma_0)$ and $p^1 \in L^2(\Gamma_0, H^1_{\#(1,2)}(Y^*))$ and the analogous ansatz for the test field q^ε; on considering extension of gradient$(\partial_\alpha^y, \partial_z)$ by zero in $Y \setminus Y^*$, at the ε^0 order we obtain (note $\int_\Omega = \int_{\Gamma_0 \times Y}$)

$$c^2 \int_{\Gamma_0 \times Y^*} \left(\partial_\alpha^x p^0 + \partial_\alpha^y p^1\right)\left(\partial_\alpha^x q^0 + \partial_\alpha^y q^1\right) + c^2 \frac{1}{\varkappa^2} \int_{\Gamma_0 \times Y^*} \partial_z p^1 \partial_z q^1 - \omega^2 \int_{\Gamma_0 \times Y^*} p^0 q^0$$
$$= \frac{1}{\varkappa} \int_{\Gamma_0} \left[g^{0+} \int_{I_y^+} q^1 \, \mathrm{d}\Gamma_y + g^{0-} \int_{I_y^-} q^1 \, \mathrm{d}\Gamma_y \right]. \tag{11}$$

By choosing subsequently combinations of either $q^0 = 0$, or $q^1 = 0$ we get the local, or the global subproblems, respectively; from the local one due to the linearity we introduce the decomposition (recall $g^0 = g^{0+} = -g^{0-}$)

$$p^1(x_\alpha, y) = \pi^\beta(y) \partial_\beta^x p^0(x_\alpha) + \mathrm{i}\omega \xi(y) g^0(x_\alpha), \tag{12}$$

where *corrector basis functions* $\pi^\beta, \xi \in H^1_{\#(1,2)}(Y)/\mathbb{R}$, $\beta = 1, 2$ are solutions of the local auxiliary problems:

$$\int_{Y^*} \partial_\alpha^y (y^\beta + \pi^\beta) \, \partial_\alpha^y q + \frac{1}{\varkappa^2} \int_{Y^*} \partial_z \pi^\beta \partial_z q = \int_{Y^*} \hat{\nabla}_y (y^\beta + \pi^\beta) \cdot \hat{\nabla}_y q = 0, \tag{13}$$

for all $q \in H^1_{\#(1,2)}(Y)/\mathbb{R}$, $\beta = 1, 2$, and

$$\int_{Y^*} \left[\partial_\alpha^y \xi \, \partial_\alpha^y q + \frac{1}{\varkappa^2} \partial_z \xi \, \partial_z q \right] = \int_{Y^*} \hat{\nabla}_y \xi \cdot \hat{\nabla}_y q = -\frac{|Y|}{c^2 \varkappa} \left(\int_{I_y^+} q - \int_{I_y^-} q \right), \tag{14}$$

for all $q \in H^1_{\#(1,2)}(Y)/\mathbb{R}$.

Step 3: We introduce the gradient $\Xi^\varepsilon = \hat{\nabla}^\varepsilon p^\varepsilon = (\partial_\alpha^x p^\varepsilon, \frac{1}{\varkappa\varepsilon} \partial_z p^\varepsilon)$ and denote by $\hat{\Xi}^\varepsilon$ its extension by *zero* to entire Ω. Using the a priori estimates one obtains $\hat{\Xi}^\varepsilon \rightharpoonup \hat{\Xi}^0$ weakly in $L^2(\Omega)$. Then the use of special test functions yields the relationships of tangent and normal components of limit gradient $\hat{\Xi}^0$; while $\hat{\Xi}^0_\alpha$ is involved in the global equation governing tangent acoustic wave propagation

$$c^2 \int_{\Gamma_0} \left(\int_{-1/2}^{1/2} \hat{\Xi}^0_\alpha \mathrm{d}z \right) \partial_\alpha^x \bar{q} - \omega^2 \frac{|Y^*|}{|Y|} \int_{\Gamma_0} p^0 \bar{q} = 0 \quad \forall \bar{q} \in H^1(\Gamma_0), \tag{15}$$

$\hat{\Xi}^0_z$ is involved in the transversal transmission relationship

$$c^2 \int_{\Gamma_0} \int_{-1/2}^{1/2} \hat{\Xi}^0_z \psi = -\mathrm{i}\omega \int_{\Gamma_0} g^0 \left(\int_0^{1/2} \psi(x_\alpha, \zeta) \, \mathrm{d}\zeta - \int_0^{-1/2} \psi(x_\alpha, \zeta) \, \mathrm{d}\zeta \right), \tag{16}$$

for all $\psi \in \mathcal{D}(\Gamma_0; L^1(I_z))$. Hence for $\psi(x_\alpha, z) = \bar{\varphi}(x_\alpha) \in \mathcal{D}(\Gamma_0)$, we obtain $c^2 \int_{-1/2}^{1/2} \hat{\Xi}^0_z = -\mathrm{i}\omega g^0$.

In order to identify the limit gradient the Tartar method is used. First in (5) we apply test function $q^\varepsilon = \tilde{w}^\varepsilon_\alpha \varphi$, where $\tilde{w}^\varepsilon_\alpha = \varepsilon \mathcal{P}_\Omega(\pi^\alpha(x/\varepsilon)) + x_\alpha$ and $\varphi \in \mathcal{D}(\Gamma_0)$; obviously, such φ are embedded in $H^1(\Omega)$ with $\partial_z \varphi = 0$. From the resulting identity we subtract the local problem (13) rewritten in the following global form

$$\int_\Omega \hat{\nabla}^\varepsilon \tilde{w}^\varepsilon_\alpha \cdot \hat{\nabla}^\varepsilon \phi = 0 \quad \forall \phi \in H^1_0(\Gamma_0; H^1(I_z)) \tag{17}$$

and evaluated for $\phi = \varphi \tilde{p}^\varepsilon$. This subtraction eliminates an undesired term for which the convergence is not known. The remaining terms converge due to (9), so that we obtain

$$c^2 \int_\Omega \hat{\Xi}^0 \cdot (x_\alpha \hat{\nabla} \varphi) - c^2 \int_{\Gamma_0} \mathcal{M}_Y(\partial_\beta^y \tilde{w}_\alpha) \partial_\beta \varphi p^0 - \omega^2 \int_\Omega p^0 x_\alpha \varphi = \frac{\mathrm{i}\omega}{\varkappa} \int_{\Gamma_0} g^0 \left[\int_{I_y^+} \pi^\alpha - \int_{I_y^-} \pi^\alpha \right] \varphi \frac{1}{|I_y|} \mathrm{d}\Gamma, \tag{18}$$

where $\mathcal{M}_Y(\phi) = |Y|^{-1} \int_{Y^*} \phi$ is the mean. Since $\partial_z \varphi = 0$ and because $\mathcal{M}_Y(\partial_\beta^y \tilde{w}_\alpha)$ is constant, integration by parts in (18) yields

$$c^2 \int_{-1/2}^{1/2} \hat{\Xi}^0_\alpha \, \mathrm{d}z = c^2 \mathcal{M}_Y(\partial_\beta^y \tilde{w}_\alpha) \partial_\beta^x p^0 + \frac{\mathrm{i}\omega}{\varkappa} g^0 \frac{1}{|I_y|} \left[\int_{I_y^+} \pi^\alpha - \int_{I_y^-} \pi^\alpha \right], \tag{19}$$

where the homogenized gradient is identified:

$$c^2 \int_{-1/2}^{1/2} \hat{\Xi}_\alpha^0 \, \mathrm{d}z = A_{\alpha\beta} \partial_\beta^x p^0 + \mathrm{i}\omega B_\alpha g^0,$$

$$\text{where} \quad A_{\alpha\beta} = c^2 \mathcal{M}_Y(\partial_\beta^y \tilde{w}_\alpha) = c^2 \frac{1}{|Y|} \int_{Y^*} \left(\partial_\beta^y \pi^\alpha + \delta_{\alpha\beta} \right), \tag{20}$$

$$B_\alpha = \frac{1}{\varkappa |I_y|} \left[\int_{I_y^+} \pi^\alpha - \int_{I_y^-} \pi^\alpha \right] \mathrm{d}\Gamma.$$

Using $(20)_1$ substituted in (15) we obtain the tangent wave propagation relationship:

$$\int_{\Gamma_0} \left(A_{\alpha\beta} \partial_\beta^x p^0 + \mathrm{i}\omega B_\alpha g^0 \right) \partial_\alpha^x \bar{q} - \omega^2 \frac{|Y^*|}{|Y|} \int_{\Gamma_0} p^0 \bar{q} = 0 \quad \forall \bar{q} \in H^1(\Gamma_0). \tag{21}$$

We follow an analogical procedure involving the second auxiliary problem (14) rewritten in the global form for $\xi^\varepsilon(x) = \varepsilon \xi(x/\varepsilon)$ (gradients extended by zero from $\Omega^{*\varepsilon}$ to entire Ω)

$$c^2 \int_\Omega \hat{\nabla}^\varepsilon \xi^\varepsilon \cdot \hat{\nabla}^\varepsilon q = -\frac{|Y|}{\varkappa} \left(\int_{\Gamma^+} q - \int_{\Gamma^-} q \right), \tag{22}$$

where we substitute $q = \tilde{p}^\varepsilon \varphi$, $\varphi \in \mathcal{D}(\Gamma_0)$ and use $\hat{\Xi}^\varepsilon = \hat{\nabla}^\varepsilon p^\varepsilon$. On subtracting the resulting identity from (5) where $q := \varphi \xi^\varepsilon$, we may pass in the limit with all terms (obviously $\xi^\varepsilon \to 0$ strongly in $L^2(\Omega)$), thus, we obtain

$$c^2 \int_{\Gamma_0} \frac{1}{|Y|} \int_{Y^*} (\partial_\alpha^y \xi) \, p^0 \partial_\alpha^x \varphi = -\frac{\mathrm{i}\omega}{\varkappa} \int_{\Gamma_0} \varphi g^0 \left(\int_{I_y^+} \xi - \int_{I_y^-} \xi \right) + \frac{|Y|}{\varkappa} \int_{\Gamma_0} \varphi (p^+ - p^-), \tag{23}$$

where p^+ and p^- are the traces on Γ_0 of the pressure fields from domains Ω^+ and Ω^-, respectively, see (10). On integrating by parts, since $\partial_z \varphi = 0$, and multiplying by $\varkappa/|I_y|$ we get

$$\int_{\Gamma_0} D_\alpha \partial_\alpha^x p^0 \varphi + \mathrm{i}\omega \int_{\Gamma_0} g^0 F \varphi = \int_{\Gamma_0} \varphi (p^+ - p^-), \tag{24}$$

(note $|Y| = |I_y|$), where the homogenized coefficients are defined as follows

$$D_\alpha = c^2 \frac{\varkappa}{|I_y|} \mathcal{M}_Y(\partial_\alpha^y \xi), \qquad F = \frac{1}{|I_y|} \left(\int_{I_y^+} \xi - \int_{I_y^-} \xi \right). \tag{25}$$

There is the following relationship

$$B_\beta = \frac{1}{\varkappa} D_\beta, \tag{26}$$

which follows on substituting $q := \pi^\beta$ in (14) and $q := \xi^\pm$ in (13).

Step 4: Let us consider $\varepsilon_0 > 0$ characterizing a finite thickness of the transmission layer. For coupling the homogenized transmission layer model with the global problem imposed in Ω^G, in (10) we evaluated the traces of the acoustic pressure on both faces of the limit interface, $\Gamma_0^\pm$. Given thickness $\delta_0 > 0$ the l.h.s. in (10) can also be written as $\delta_0 \int_\Omega \phi \partial_3 \widetilde{p^{\varepsilon_0 \delta_0}}$ (we recall the use of smooth extension $\widetilde{p^{\varepsilon_0 \delta_0}}$ to entire Ω_{δ_0}). We employ the asymptotic expansion ansatz, see Step 2 above, $\widetilde{p^\varepsilon}(x) = p^0(x_\alpha) + \varepsilon \widetilde{p^1}(x_\alpha, y) + \dots$, where $\widetilde{p^1}(x_\alpha, \cdot) \in H^1_{\#(1,2)}(Y)$, and consider the following approximation for $\varepsilon < \varepsilon_0$:

$$\begin{aligned} \delta_0 \int_\Omega \phi \partial_3 \widetilde{p^{\varepsilon_0 \delta_0}} \approx \quad & \varepsilon_0 \int_\Omega \frac{1}{\varepsilon} \phi \frac{\partial \widetilde{p^\varepsilon}}{\partial z} = \varepsilon_0 \int_{\Gamma_0} \frac{\phi}{\varepsilon} \frac{\partial}{\partial z} \left(\varepsilon \widetilde{p^1}(x_\alpha, y) + \varepsilon^2 \cdots \right) \\ \stackrel{\varepsilon \to 0}{\longrightarrow} \; & \varepsilon_0 \int_{\Gamma_0} \mathcal{M}_Y \left(\frac{\partial \widetilde{p^1}}{\partial z} \right) = \varepsilon_0 \int_{\Gamma_0} \phi \frac{1}{|I_y|} \left[\int_{I_y^+} p^1 \, \mathrm{d}\Gamma_y - \int_{I_y^-} p^1 \, \mathrm{d}\Gamma_y \right], \end{aligned} \tag{27}$$

for all $\phi \in L^2(\Gamma_0)$, where the transversal Y-periodicity of $\widetilde{p^1}(x_\alpha, \cdot)$ was employed. Thus, we may express the pressure jump in (10) by the 1st order approximation in the transmission layer using (27)

$$\begin{aligned} \frac{1}{\varepsilon_0} \int_{\Gamma_0} \phi (p^+ - p^-) & \approx \int_{\Gamma_0} \phi \frac{1}{|I_y|} \left[\int_{I_y^+} p^1 \, \mathrm{d}\Gamma_y - \int_{I_y^-} p^1 \, \mathrm{d}\Gamma_y \right] \\ & = \int_{\Gamma_0} \phi \left(\varkappa B_\alpha \partial_\alpha^x p^0 + \mathrm{i}\omega F g^0 \right), \end{aligned} \tag{28}$$

where the decomposed form of p^1 defined in (12) was used. Due to (26), Eq. (24) is recovered up to the scaling factor of $1/\varepsilon_0$. It is worth to remark that (28) could be obtained quite naturally using the *unfolding method of homogenization*. Instead of (24), in what follows, we shall consider the approximation defined by (28) as the relevant relationship, where $\approx$ is replaced by $=$.

3.2. Limit macroscopic problem in the transmission layer

We shall now summarize the homogenization result derived in the previous section. Homogenized transmission problem is expressed in terms of *interface mean acoustic pressure* $p^0 \in H^1(\Gamma_0)$, and *fictitious acoustic transverse velocity* $g^0 \in L^2(\Gamma_0)$; these quantities satisfy the interface problem constituted by (21) and (28) multiplied by i ω:

$$
\begin{aligned}
&\int_{\Gamma_0} A_{\alpha\beta}\partial_\beta^x p^0 \partial_\alpha^x q - \frac{|Y^*|}{|Y|}\omega^2 \int_{\Gamma_0} p^0 q + \mathrm{i}\omega \int_{\Gamma_0} B_\alpha \partial_\alpha^x q\, g^0 = 0,\\
&-\mathrm{i}\omega \int_{\Gamma_0} D_\beta \partial_\beta^x p^0 \psi + \omega^2 \int_{\Gamma_0} F g^0 \psi = -\mathrm{i}\omega \frac{1}{\varepsilon_0}\int_{\Gamma_0} (p^+ - p^-)\psi,
\end{aligned}
\tag{29}
$$

for all $q \in H^1(\Gamma_0)$ and $\psi \in L^2(\Gamma_0)$. These equations involve the homogenized coefficients $A_{\alpha\beta}$, B_α, D_α and F expressed in terms of the local corrector functions π^β and ξ; using (13) a symmetric form of $A_{\alpha\beta}$ in $(20)_2$ can be obtained, so that from (20) and (25) we have

$$
\begin{aligned}
A_{\alpha\beta} &= \frac{c^2}{|Y|}\int_{Y^*} \partial_\gamma^y (y^\beta + \pi^\beta)\,\partial_\gamma^y (y^\alpha + \pi^\alpha) + \frac{c^2}{|Y|\varkappa^2}\int_{Y^*} \partial_z \pi^\beta \partial_z \pi^\alpha,\\
B_\alpha &= \frac{1}{\varkappa |I_y|}\left(\int_{I_y^+} \pi^\alpha - \int_{I_y^-} \pi^\alpha\right), \qquad D_\alpha = \frac{c^2\varkappa}{|Y|}\int_{Y^*} \partial_\alpha^y \xi,\\
F &= \frac{1}{|I_y|}\left(\int_{I_y^+} \xi - \int_{I_y^-} \xi\right).
\end{aligned}
\tag{30}
$$

We remark that p^0 presents an internal variable describing the acoustic wave distributed in the interface layer, being driven by g^0; this phenomenon is featured by $\partial_\alpha p^0 \neq 0$ and it appears only if the coupling coefficients do not vanish, i.e. $B_\beta, D_\beta \neq 0$, see Section 5. Below we shall introduce an effective *acoustic impedance* X involved in $p^+ - p^- = X g^0$ which relates the pressure jump on Γ_0 to the transverse velocity represented by g^0, see also Fig. 1. In Section 4.1, by virtue of the finite element method we compute an approximation to X.

4. Global problem of acoustic wave transmission

The transmission conditions on interface Γ_0 defined in (2) can now be replaced by the homogenized interface problem (29) which makes the relationship between couple (p^0, g^0) and the pressure jump, $p^+ - p^-$. Thus, instead of (2), we shall consider (normals n^+ and n^- are defined as in (2))

$$
c^2 \frac{\partial p^+}{\partial n^+} = \mathrm{i}\omega g^0 \quad \text{on } \Gamma_0, \qquad c^2 \frac{\partial p^-}{\partial n^-} = -\mathrm{i}\omega g^0 \quad \text{on } \Gamma_0. \tag{31}
$$

4.1. Discretized interface problem

Interface layer pressure p^0 can be eliminated from the coupled transmission problem approximated by the finite element method. We consider discretized interface surface (or line in 2D) Γ_{0h}. Let $\mathbf{p}^0$, $\mathbf{p}^\pm$ and $\mathbf{g}^0$ be the column vectors of the FE approximation to p^0, $p^\pm$ and g^0, respectively, and the integrals in (29) are approximated as follows (notation $\mathbf{p}^H$ means the Hermitian transpose to $\mathbf{p}$)

$$
\begin{aligned}
&\int_{\Gamma_0} A_{\alpha\beta}\partial_\beta^x p \partial_\alpha^x q \approx \mathbf{q}^H \mathbf{A}\mathbf{p}, \qquad \int_{\Gamma_0} pq \approx \mathbf{q}^H \mathbf{M}\mathbf{p}, \qquad \int_{\Gamma_0} F g^0 \psi \approx \boldsymbol{\psi}^H \mathbf{F}\mathbf{g}^0,\\
&\int_{\Gamma_0} B_\alpha \partial_\alpha^x q g^0 \approx \mathbf{q}^H \mathbf{B}\mathbf{g}^0, \qquad \int_{\Gamma_0} D_\alpha \partial_\alpha^x p \psi \approx \boldsymbol{\psi}^H \mathbf{D}\mathbf{p}.
\end{aligned}
$$

Using this self-explaining notation, the FE approximated problem (29) is written as

$$
\begin{aligned}
&\mathbf{A}\mathbf{p}^0 - \phi^* \omega^2 \mathbf{M}\mathbf{p}^0 + \mathrm{i}\omega \mathbf{B}^{\mathrm{T}}\mathbf{g}^0 = 0,\\
&-\mathrm{i}\omega \mathbf{D}\mathbf{p}^0 + \omega^2 \mathbf{F}\mathbf{g}^0 = -\mathrm{i}\omega \mathbf{M}(\mathbf{p}^+ - \mathbf{p}^-)\frac{1}{\varepsilon_0}.
\end{aligned}
$$

Table 1
Homogenized coefficients for perforations #1, #2, #3. D defined by (26) with $\varkappa = 1$.

Mic.	A ((m/s)^2)	B (m)	F (s^2)
#1	1.155×10^5	0	1.391×10^{-5}
#2	1.704×10^5	−0.251	1.324×10^{-5}
#3	2.186×10^5	−0.897	4.265×10^{-5}

On computing the Schur complement (for ω out-of-resonance), it is possible to introduce the *coupled impedance*

$$\mathbf{X}(\omega^2) = \omega^2[\mathbf{F} - \mathbf{D}(\mathbf{A} - \phi^*\omega^2\mathbf{M})^{-1}\mathbf{B}^{\mathrm{T}}], \tag{32}$$

hence the discretized interface transmission condition reduces to

$$\varepsilon_0\mathbf{X}(\omega^2)\mathbf{g}^0 = -\mathrm{i}\omega\mathbf{M}(\mathbf{p}^+ - \mathbf{p}^-), \tag{33}$$

which resembles the structure of the standard conditions (2), since $\mathbf{g}^0$ approximates the transverse velocities, i.e. $\mathbf{g}^0 \approx \partial p^+/\partial n^+ = -\partial p^-/\partial n^-$.

4.2. The acoustic problem in a duct with perforated obstacles—Weak formulation

As explained above, in domains with a perforated obstacle Γ_0 the acoustic pressure is discontinuous along Γ_0, which in general can be a fissure embedded in a connected domain Ω^G. For this we need $H^1_{-1}(\Omega^G, \Gamma_0)$, the space of discontinuous solutions defined at once in the whole of Ω^G : $H^1_{-1}(\Omega^G, \Gamma_0) = \{q \in L^2(\Omega^G) : q|_{\Omega^r} \in H^1(\Omega^r), r = +, -\}$. By $q^+ = \gamma^+(q)$ and $q^- = \gamma^-(q)$ we denote traces on Γ_0 of $q \in H^1(\Omega^+)$ and $q \in H^1(\Omega^-)$, respectively. Thus, in what follows by p we denote the solution in $\Omega \subset \Gamma_0$, whereas on Γ_0 the pressure is introduced by traces p^+ and p^- of $p \in H^1(\Omega^+)$ and $p \in H^1(\Omega^-)$, respectively; these traces are involved in the interface problem (29).

We also need to specify boundary conditions on boundary $\partial\Omega^G = \Gamma_{\mathrm{in}} \cup \Gamma_{\mathrm{out}} \cup \Gamma_{\mathrm{w}}$ consisting of the planar surfaces Γ_{in}, Γ_{out} and the channel walls Γ_{w}, see Fig. 1. On Γ_{in} we assume an incident wave of the form $\tilde{p}(x, t) = \bar{p}\mathrm{e}^{-\mathrm{i}kn_l \cdot x_l}\mathrm{e}^{\mathrm{i}\omega t}$, where (n_l) is the outward normal vector of Ω^G, on Γ_{out} we impose the radiation condition in the form of the anechoic output, so that

$$\begin{aligned} &\mathrm{i}\omega p + c\frac{\partial p}{\partial n} = 2\mathrm{i}\omega\bar{p} \quad \text{on } \Gamma_{\mathrm{in}}, \\ &\mathrm{i}\omega p + c\frac{\partial p}{\partial n} = 0 \quad \text{on } \Gamma_{\mathrm{out}}, \\ &\frac{\partial p}{\partial n} = 0 \quad \text{on } \Gamma_{\mathrm{w}}. \end{aligned} \tag{34}$$

Given amplitude $\bar{p}$ of incident plane wave with frequency ω, the weak solution $p \in H^1_{-1}(\Omega^G, \Gamma_0)$ to our acoustic problem is obtained by

$$c^2\int_{\Omega^G} \nabla p \cdot \nabla q - \omega^2\int_{\Omega^G} pq + \mathrm{i}\omega c\int_{\Gamma_{\mathrm{in}}\cup\Gamma_{\mathrm{out}}} pq\,\mathrm{d}\Gamma - \int_{\Gamma_0^+} g^0 q^+\,\mathrm{d}\Gamma + \int_{\Gamma_0^-} g^0 q^-\,\mathrm{d}\Gamma = \mathrm{i}2\omega c\int_{\Gamma_{\mathrm{in}}} \bar{p}q\,\mathrm{d}\Gamma, \tag{35}$$

$\forall q \in H^1_{-1}(\Omega^G, \Gamma_0)$, where $q^{+/-} = \gamma^{+/-}(p)$ are the traces on Γ_0 and g^0 is the solution of interface problem (29). In (35) we employed conditions (31).

5. Numerical examples

Examples introduced in this section were computed using our code based on the Matlab system. We use Q1 finite element approximation for acoustic pressure in Ω^G and P1 line elements on Γ_0 to approximate p^0 and g^0. The numerical examples are aimed to illustrate how the "global response" presented by the acoustic pressure filed in a duct is sensitive to the type of perforation.

5.1. Homogenized coefficients for various perforations

In Fig. 4, we display corrector functions ξ for three different perforations (microstructures Mic. #1,#2,#3); the corresponding homogenized coefficients are in Table 1. Due to the geometrical arrangement of the solid obstacles the coupling coefficients B, D vanish for perforation type #1. For types #2 and #3, these coefficients are nonzero, i.e. the transverse and the tangential velocities in the interface layer are coupled.

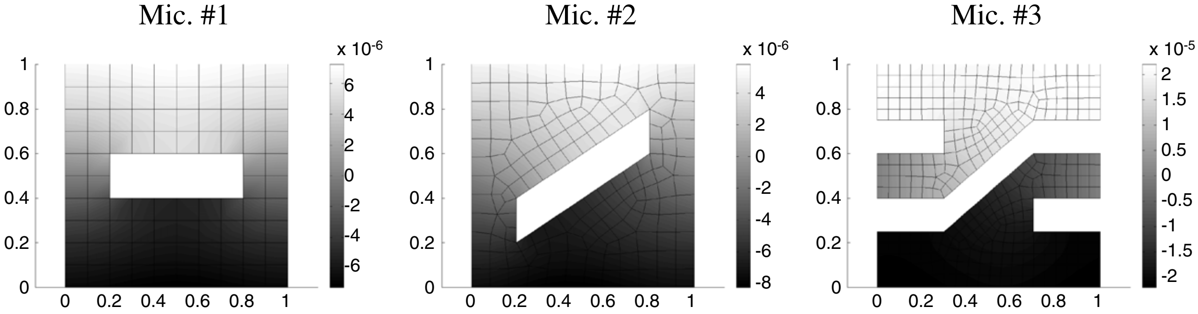

Fig. 4. Distribution of ξ in Y^*.

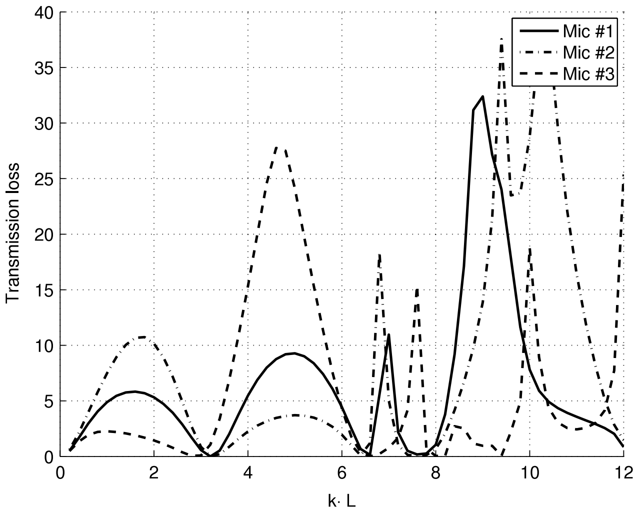

Fig. 5. Transmission losses for different perforation types.

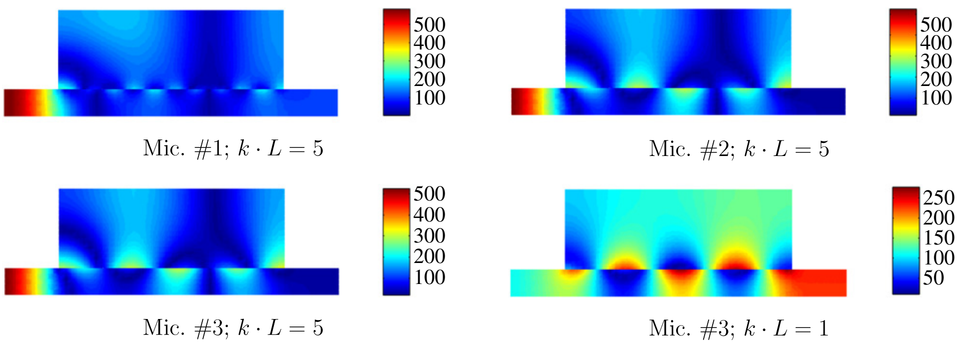

Fig. 6. Modulus of the acoustic pressure in Ω for $k \cdot L = 5$ (1 in the last picture). For this 2D computation a finite element mesh comprising 820 quadrilateral elements was used.

5.2. Modelling an acoustic waveguide

This numerical example shows the global response of a waveguide with the homogenized transmission layer. The geometry of the waveguide is depicted in Fig. 1. The global response can be characterized by the transmission loss $TL = 20 \log \left(|\bar{p}_{|\Gamma_{\mathrm{in}}}| / |p_{|\Gamma_{\mathrm{out}}}| \right)$, where $\bar{p}$ is the incident plane wave, see (34). The transmission losses for the waveguide with perforations #1, #2 and #3 are shown in Fig. 5. On the horizontal axis there is the wave number k ($k = \omega/c$) multiplied by length L of the "expansion chamber" (see Fig. 1, right). The resulting acoustic pressures in the waveguide are displayed in Fig. 6. The numerical results were obtained for acoustic speed $c = 343$ m/s and scale parameter $\varepsilon_0 = 0.035$, which e.g. for type #1 means that the thickness of the perforated plate is 7 mm.

6. Conclusion

The transmission conditions discussed in this paper involve homogenized parameters which reflect specific features of the periodic perforation. The perforated barriers can have quite general structures, thus, not only flat plates with holes, but very complicated geometries may be considered. Moreover, even the "no-obstacle" situation is treated by the present model, when $Y = Y^*$ and $\varkappa \to +\infty$. Indeed, then $\pi^\beta = \xi \equiv 0$, therefore both F and D_β vanish, so that $(29)_2$ yields continuity $p^+ = p^-$ on Γ_0.

In this paper the asymptotic analysis based on the Tartar method of oscillating test functions was reported briefly in Section 3; details on the a priori estimation and convergence proofs based on the *periodic unfolding method* will be published in a forthcoming paper. We recall that most recently a different homogenization approach was used in papers [3,2], however there the result is applicable merely to "flat" designs of the perforation, thus disregarding the effects of an interaction between transversal and the induced tangent waves.

The numerical study reported in Section 5 shows that the global response is very sensitive to the perforation design. Even though the porosity was almost the same for all designs (0.4 for #1,#2 and ≈0.4 for #3, but this parameter is not well defined), there are big differences in the acoustic pressure distributions and also in the transmission losses.

We emphasize that this modelling tool allows for the formulation and treatment of the "optimal perforation design", which can be another extension of the structural optimization in acoustics (see e.g. [10]); this will be pursued in further studies.

References

[1] R. Kirby, A. Cummings, The impedance of perforated plates subjected to grazing gas flow and backed by porous media, J. Sound Vibration 217 (4) (1998) 619–636.
[2] A.S. Bonnet-Bendhia, D. Drissi, N. Gmati, Mathematical analysis of the acoustic diffraction by a muffler containing perforated ducts, Math. Models Methods Appl. Sci. 15 (7) (2005) 1059–1090.
[3] A.S. Bonnet-Bendhia, D. Drissi, N. Gmati, Simulation of muffler's transmission losses by a homogenized finite element method, J. Comput. Acoust. 12 (3) (2004) 447–474.
[4] C. Conca, Étude d'un fluid traversant une paroi perforée, I. Comportement limite près de la paroi, J. Math. Pures Appl. 66 (1987) 1–43.
[5] J. Sanchez-Hubert, E. Sanchez–Palencia, Acoustic fluid flow through holes and permeability of perforated walls, J. Math. Anal. Appl. 87 (1982) 427–453.
[6] D. Cioranescu, J. Saint Jean Paulin, Homogenization of Reticulated Structures, in: Appl. Math. Ser., vol. 136, Springer, New York, 1999.
[7] D. Cioranescu, A. Damlamian, G. Griso, Periodic unfolding and homogenization, C. R. Acad. Sci. Paris, Ser. I 335 (2002) 99–104.
[8] D. Cioranescu, A. Damlamian, G. Griso, D. Onofrei, The periodic unfolding method for perforated domains and Neumann sieve models, J. Math. Pures Appl. 89 (2008) 248–277.
[9] A. Ávila, G. Griso, B. Miara, E. Rohan, Multiscale modeling of elastic waves: Theoretical justification and numerical simulation of band gaps, Multiscale Model. Simul. SIAM 7 (2008) 1–21.
[10] E. Bangtsson, D. Noreland, M. Berggren, Shape optimization of an acoustic horn, Comput. Methods Appl. Mech. Engrg. 192 (2003) 1533–1571.
[11] E. Sanchez–Palencia, Non-Homogeneous Media and Vibration Theory, in: Lecture Notes in Physics, vol. 127, Springer, Berlin, 1980.